Optical Characterization of High Refractive Index Glass Wafers for Augmented Reality Wearables

Jue Wang [1*], Michael J. Cangemi [1], Jean Francois Oudard [1], Alex Bean [1], Tom J. Dunn [1], Chris A. Lee [1], Deanna A. Moschitta [2], Michael J. Moore [2], Nicholas M. Walker [2], Michael A. Kapusta [2], Karl W. Koch [2]

[1]*Corning Advanced Optics, Corning Incorporated. 60 O'Connor Road, Fairport, New York 14450, USA*
[2]*Corning Sullivan Park, Corning Incorporated. 1 Science Drive, Corning, New York, 14831, USA*
*wangj3@corning.com

Abstract: Refractive index and optical thickness homogeneities of 99.979% and 99.984% were determined by using wafer-size metrologies. SiO_2 & Nb_2O_5 based low loss anti-reflective coatings in the visible were realized for augmented reality wearables.

OCIS codes: (310.3840) Materials and process characterization; (310.1210) Antireflection coatings

1. Introduction

Glass is one of the world's most transformative materials [1]. Corning's augmented reality solution integrates high refractive index glass wafers with high optical transmission and exceptional flatness [2], high-throughput metrology expertise [3], and fully automated laser cutting technology [4]. Advantages of the glass wafers include high transparency, low birefringence, high refractive index (≥ 1.7), high durability, optical quality, low total thickness variation, high mechanical stability, stiffness, and better geometrical stability [2]. Anti-reflective coatings in the visible brings additional benefit to augmented reality wearables.

Augmented reality (AR) wearables, such as smart glasses, enable users to see computer-generated images overlaid on top of the real world [5, 6]. This enables an enhanced experience for users in activities they normally perform with the aid of a computer or mobile phone. For example, AR wearables can allow maintenance personnel to troubleshoot in a hands-free fashion. Multiple optical architectures exist – waveguides, reflective combiners, and beam splitters (a.k.a. bird bath designs) – for making AR wearables [7~9]. Each of these architectures has varying degrees of advantage in form factor (size and weight), visual comfort, optical quality, and cost. No existing architecture is advantaged in all of these areas without tradeoffs. We believe a sleek and light form factor is critical for broad market adoption, and waveguide technology is the most advantaged. Waveguide technology uses a combination of diffractive gratings and high index glass lenses to transfer images from the light source (projector) to the user's eye through Total Internal Reflection (TIR).

For the realization of the waveguide based devices, several high refractive glasses were developed. The refractive indices of the glass wafers increase to 1.7, 1.8 and 1.9, corresponding to Corning Glass Code (CGC) 70035, 80235 and 80230. This paper reports the refractive index homogeneity and optical total thickness variation of high refractive index glass wafers evaluated by using wafer-size metrologies. Optical dispersions of the high refractive index glass wafers are generated. A set of low refractive index and high refractive index single-layer coatings are evaluated with top-down as well as upside-down configuration. Results of an anti-reflective coating are presented.

2. Optical Characterization of Uncoated High Refractive Index Glass Wafers

A variable angle spectroscopic ellipsometer (VASE) Woollam model M-2000 was employed to evaluate the refractive index homogeneity of the high refractive index glass wafers. The M-2000 ellipsometer equipped with a rotating compensator ellipsometry (RCE) technology and a high-speed CCD detection provides wafer-size uniformity mapping capabilities [10]. Table 1 highlights the minimum and maximum refractive indices derived from the M-2000 ellipsometric mapping over ϕ100 mm CGC 70035 glass wafers with a step separation of 10 mm between nearest measurement spots. The average refractive index homogeneity of 99.979% was obtained from the refractive index variation across the whole wafers. It is worth noting that the M-2000 ellipsometer simultaneously captures a broad spectral range from deep ultraviolet to near infrared. The refractive indices at a wavelength of 460 nm were selected to calculate the homogeneity.

A frequency stepping interferometer, Corning Tropel's Flatmaster™ MSP-300, was used to simultaneously capture the optical total thickness variation over the whole glass wafers. The MSP-300 multi-surface profiler provides a fast and accurate metrology for a glass wafer size up to ϕ300 mm [11]. Table 2 lists the optical thickness homogeneities over ϕ100 mm CGC 70035 glass wafers. The average optical thickness homogeneity of 99.984% was obtained from the optical thickness variation across the entire wafers. The MSP-300 multi-surface profiler characterized the optical thickness homogeneity and is consistent with the M-2000 ellipsometer measured refractive index homogeneity. It is worth noting that the MSP-300 presents some metrology advantages for the glass wafer homogeneity evaluation compared to the M-2000 ellipsometer. The MSP-300 collects three million data points in seconds with sub-micron accuracy enabling total optical thickness and flatness characterization over the entire surface [11]. The M-2000 ellipsometer, on the other hand, maps the wafer surface point by point. In addition, the ellipsometer indirectly measures the refractive index, by measuring the ratio changes of different reflective polarizations. As a result, the ellipsometry is sensitive to sample surface quality and requires sophisticated modeling skill [12].

Table 1. Refractive index homogeneities of CGC 70035 glass wafers via M-2000 mapping.

Glass Wafer ID	Minimum Refractive Index at 460 nm	Maximum Refractive Index at 460 nm	Refractive Index Homogeneity (%)
18-2018_100	1.7248	1.7251	99.978
18-2018_101	1.7242	1.7246	99.978
18-2018_102	1.7245	1.7248	99.980

Table 2. Optical thickness homogeneity of CGC 70035 glass wafers via MSP-300 at a wavelength of 830 nm.

Glass Wafer ID	Average Optical Thickness (µm)	Maximum Optical Thickness Variation (µm)	Optical Thickness Homogeneity (%)
18-2012_098	558.94	0.08125	99.985
18-2012_099	559.25	0.08775	99.984
18-2012_100	559.45	0.09425	99.983

The M-2000 ellipsometer was used to generate optical dispersions of the high refractive index glass wafers. For the amorphous glass wafers, a Tauc-Lorentz model was selected to fit backside-corrected ellipsometric data. Fig. 1 plots generated dispersion of ϕ150 mm x 325 µm double side polished CGC 80235 wafer, along with measured & modeled transmission. It is worth noting that the glass wafer is absorption free in the visible. Absorption appears on the glass wafer at wavelengths below 350 nm. The refractive index and extinction coefficient of the glass wafer is 1.8882 and 4.9 x 10^{-6} at 350 nm, respectively.
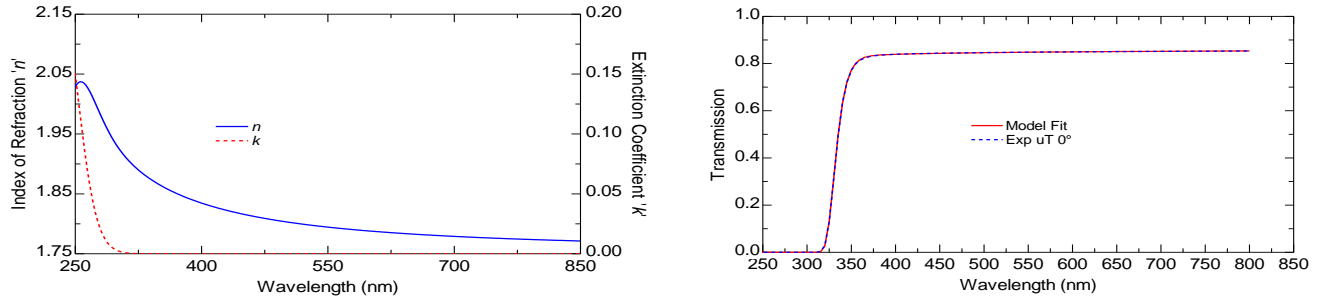

Fig. 1. Generated dispersion and measured & modeled transmission of a 325 µm thick CGC 80235 glass wafer.

3. Optical Characterization of Coated High Refractive Index Glass Wafers

High refractive index glass wafers enables wider field of view within related waveguides [13]. In addition, the high refractive indices also lead to an increase of the surface reflectance for augmented reality wearable devices. An anti-reflective coating over a broad visible spectral range is a technical solution. SiO_2 and Nb_2O_5 were selected as low and high refractive index coating materials for the demonstration of the anti-reflective coating. The M-2000 measurements were conducted on both sides of single-layer coated glass wafers. Table 3 summarizes the modeled film thickness and surface roughness in a spectral range from 300 nm to 900 nm with low values of mean-squared error (MSE) [12]. The results suggest that the ellipsometric measurement and modeling enable one to determine which side of a glass wafer was coated even without pre-coating marking.

Table 3. M-2000 modeled film thickness and surface roughness in a spectral range from 300 nm to 900 nm.

Sample Top-To-Bottom Configuration	Modeled Film Thickness (nm)	Top RMS (nm)	Mean-Squired Error (MSE)
Air/500 µm Thick Glass Wafer/85 nm SiO_2 Film/Air	86.2	0.25	2.634
Air/85 nm SiO_2 Film/500 µm Thick Glass Wafer/Air	86.0	0.42	2.542
Air/325 µm Thick Glass Wafer/160 nm Nb_2O_5 Film/Air	153.4	0.28	3.078
Air/160 nm Nb_2O_5 Film/325 µm Thick Glass Wafer/Air	153.4	0.91	3.750

Fig. 2 plots modeled dispersions of 85 nm thick SiO_2 film deposited on a ϕ150 mm x 500 µm double side polished CGC 80325 glass wafer and 160 nm thick Nb_2O_5 film deposited on a ϕ150 mm x 325 µm double side polished CGC 80325 glass wafer. In both cases, the backside correction of the ellipsometric data was considered. A Sellmeier and a Tauc-Lorentz oscillator functions were used to model the SiO_2 and Nb_2O_5 single layers with the WVASE32^{TM} software and the least root mean-squared error approach to generate the dispersions [12]. The SiO_2 film is absorption free across the spectral range with a refractive index of 1.5070 at 420 nm. For comparison, the refractive index and extinction coefficient of the Nb_2O_5 film are 2.5072 and 9.2 x 10^{-5}, respectively, at 420 nm. An anti-reflective coating was designed by using SiO_2 and Nb_2O_5 as low and

high refractive coating materials. Fig. 3 plots calculated reflectance and transmittance of the anti-reflective coating on a 325 µm thick double side polished CGC 80235 glass wafer, along with the derived absorptance of the anti-reflective coating as well as the uncoated glass wafer. An absorptance of 0.05% was realized at 420 nm for the anti-reflective coating and at 380 nm for the uncoated 325 µm thick double side polished CGC 80235 glass wafer. Such a small amount of absorptance is unmeasurable by means of standard spectrophotometers. Further absorptance reduction can be realized by either optimizing the Nb_2O_5 deposition process or using other wide bandgap oxide materials as high refractive index coating materials.
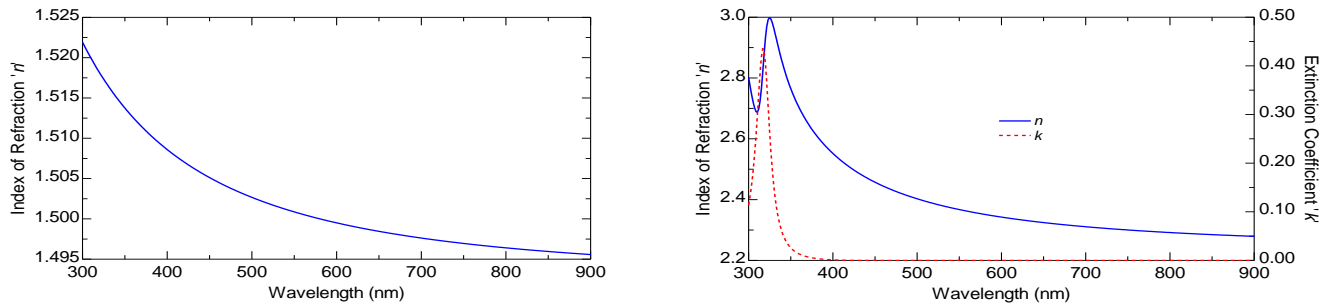

Fig. 2. Generated dispersions of 85 nm SiO_2 film (left) and 160 nm Nb_2O_5 film (right) on CGC 80235 glass wafers.
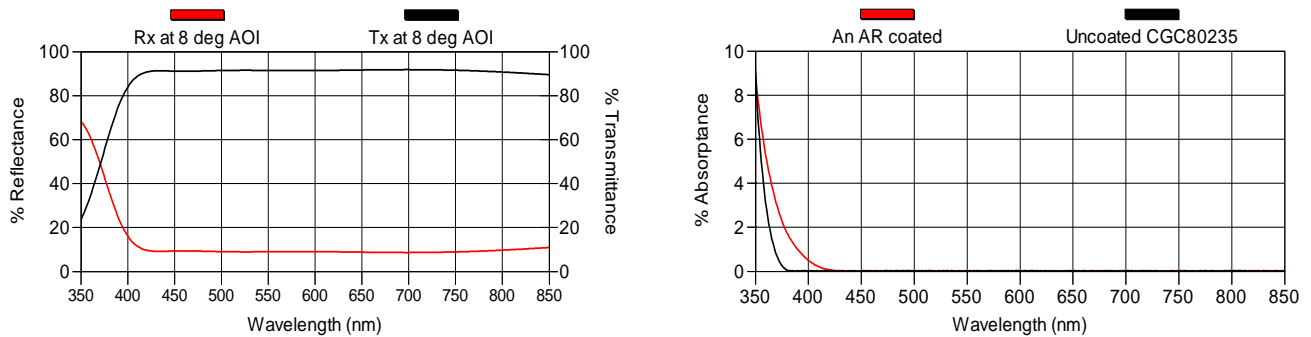

Fig. 3. Reflectance and transmittance of an anti-reflective coating deposited on 325 µm thick CGC 80235 glass wafer (left) along with derived absorptance for the AR coated wafer and uncoated wafer (right).

4. Conclusions

High quality high refractive index glass wafers enable wider field of view and enhanced waveguide effect for augmented reality wearables. A refractive index homogeneity of 99.979% and an optical thickness homogeneity of 99.984% were derived with wafer-size capable metrologies, the M-2000 and the MSP-300. M-2000 ellipsometric measurement and modeling enable one to determine which side of a glass wafer was coated without the requirement of pre-coating marking. SiO_2 and Nb_2O_5 based anti-reflective coating leads to an absorptance of 0.05% at 420 nm. Further absorptance reduction can be realized by optimizing the Nb_2O_5 deposition process or using other wide bandgap oxide materials as high refractive index coating materials.

5. References

[1] David L. Morse and Jeffrey W. Evenson, "Welcome to the Glass Age," International Journal of Applied Glass Science 7(4) 409–412 (2016). Or Corning Incorporated, "Living in the Glass Age," https://www.youtube.com/watch?v=rCFC5Lq3uSU
[2] https://www.corning.com/worldwide/en/products/advanced-optics/product-materials/specialty-glass-and-glass-ceramics/ophthalmic-glass/high-index-glass-blanks.html
[3] Robert D. Grejda, Katherine Ballman, Chris A. Lee, "Functional tolerancing using full surface metrology," Proc. SPIE 10695, Optical Instrument Science, Technology, and Applications, 106950G (28 May 2018).
[4] Anping Liu, "Advanced Laser Processing of Glass," in Conference on Lasers and Electro-Optics, OSA Technical Digest (2016) (Optical Society of America, 2016), paper STh4K.1. Or http://www.corning.com/worldwide/en/products/advanced-optics/product-materials/laser-technologies.html
[5] Tapani Levola, "Diffractive optics for virtual reality displays," Journal of the Society for Information Display 14(5), 467(2006).
[6] Nell Savage, "Augmenting reality poses challenges for optics," SPIE Professional January 2019, 28-30(2019).
[7] Sophia Chen, "More than meets the eye – augmented reality helps surgeons make decisions in real time," SPIE Professional October 2018, 24-28 (2018).
[8] Rebecca Pool, "Virtual and augmented reality tech joins the fight against crime," SPIE Professional January 2019, 16-19(2019).
[9] Stephon G. Anderson, "Wearables move beyond the consumer…and into the clinic?" SPIE Professional January 2019, 4-5(2019).
[10] https://www.jawoollam.com/products/m-2000-ellipsometer.
[11] https://www.corning.com/worldwide/en/products/advanced-optics/product-materials/analytic-instruments/metrology-instruments/tropel-flatmaster-msp-system.html.
[12] Jue Wang, Steven VanKerkhove, Horst Schreiber, "Evaluation of coated and uncoated CaF_2 optics by variable angle spectroscopic ellipsometry," Thin Solid Films 519, 2881 (2011).